

# One-laser-based generation/detection of Brillouin dynamic grating and its application to distributed discrimination of strain and temperature

Weiwen Zou,<sup>1,2,3</sup> Zuyuan He,<sup>1,4</sup> and Kazuo Hotate<sup>1,5</sup>

<sup>1</sup>Department of Electrical Engineering and Information Systems, The University of Tokyo, Tokyo 113-8656, Japan

<sup>2</sup>Currently with State Key Laboratory of Advanced Optical Communication Systems and Networks, Department of Electronic Engineering, Shanghai Jiao Tong University, Shanghai 200240, China

<sup>3</sup>wzou@sjtu.edu.cn

<sup>4</sup>zhe@ee.t.u-tokyo.ac.jp

<sup>5</sup>hotate@sagnac.t.u-tokyo.ac.jp

**Abstract:** This paper presents a novel scheme to generate and detect Brillouin dynamic grating in a polarization-maintaining optical fiber based on one laser source. Precise measurement of Brillouin dynamic grating spectrum is achieved benefiting from that the pump, probe and readout waves are coherently originated from the same laser source. Distributed discrimination of strain and temperature is also achieved with high accuracy.

©2011 Optical Society of America

**OCIS codes:** (060.2370) Fiber optics sensors; (290.5900) Scattering, stimulated Brillouin; (120.5820) Scattering measurements; (050.1950) Diffraction gratings.

---

## References and links

1. G. P. Agrawal, *Nonlinear Fiber Optics*, 3rd ed. (Academic, 2001), ch. 9.
2. K. Y. Song, W. Zou, Z. He, and K. Hotate, "All-optical dynamic grating generation based on Brillouin scattering in polarization-maintaining fiber," *Opt. Lett.* **33**(9), 926–928 (2008).
3. T. Okoshi, "Single-polarization single-mode optical fibers," *IEEE J. Quantum Electron.* **17**(6), 879–884 (1981).
4. V. P. Kalosha, W. Li, F. Wang, L. Chen, and X. Bao, "Frequency-shifted light storage via stimulated Brillouin scattering in optical fibers," *Opt. Lett.* **33**(23), 2848–2850 (2008).
5. K. Y. Song, S. Chin, N. Primerov, and L. Thévenaz, "Time-domain distributed fiber sensor with 1 cm spatial resolution based on Brillouin dynamic grating," *J. Lightwave Technol.* **28**(14), 2062–2067 (2010).
6. W. Zou, Z. He, and K. Hotate, "Complete discrimination of strain and temperature using Brillouin frequency shift and birefringence in a polarization-maintaining fiber," *Opt. Express* **17**(3), 1248–1255 (2009).
7. W. Zou, Z. He, K. Y. Song, and K. Hotate, "Correlation-based distributed measurement of a dynamic grating spectrum generated in stimulated Brillouin scattering in a polarization-maintaining optical fiber," *Opt. Lett.* **34**(7), 1126–1128 (2009).
8. W. Zou, Z. He, and K. Hotate, "Demonstration of Brillouin distributed discrimination of strain and temperature using a polarization-maintaining optical fiber," *IEEE Photon. Technol. Lett.* **22**(8), 526–528 (2010).
9. K. Y. Song, W. Zou, Z. He, and K. Hotate, "Optical time-domain measurement of Brillouin dynamic grating spectrum in a polarization-maintaining fiber," *Opt. Lett.* **34**(9), 1381–1383 (2009).

---

## 1. Introduction

Stimulated Brillouin scattering (SBS) occurs when a pump wave and a probe wave counter-propagate in an optical fiber, where the frequency of the probe is lower than that of the pump by Brillouin frequency ( $\nu_B$ ) [1]. In a polarization-maintaining optical fiber (PMF), when the pump/probe waves are linearly polarized along the same principal axis of the PMF, an acoustic grating, as so called Brillouin dynamic grating (BDG) [2], is generated associated with the SBS process. When a readout wave polarized in orthogonal to the pump/probe waves is launched into the PMF, a strong diffraction by the BDG occurs when the readout wave has a frequency deviation from the pump. The deviation is determined by the birefringence of the

PMF as  $f_{yx} = B \cdot \nu / n_{eff}$ , where  $B$  is the PMF's birefringence [3],  $n_{eff}$  the effective refractive index, and  $\nu$  the frequency of the pump wave.

The concept of the BDG has been recently adopted as an effective way to realize all-optical storage [4], high spatial-resolution time-domain distributed sensor [5], and complete discrimination of strain and temperature [6–9]. All above demonstrations [2,4–9] so far are based on using two or three laser sources to generate the pump, probe and readout waves. The accuracy of the birefringence-determined frequency deviation ( $f_{yx}$ ) is limited by relative frequency fluctuation among multiple lasers, although the accuracy could be somehow improved by time-consuming averaging process.

This paper presents, for the first time to the best of our knowledge, a successful demonstration of one-laser-based BDG generation and detection in a PMF. Superior to all BDG generation/detection schemes using multiple individual laser sources reported up to date [2,4–9], our new scheme employs only one laser source to generate the light waves to write BDG (pump and probe waves) and that to detect BDG (readout wave) by use of a sideband-generation technique. Originating from the same laser source, all three light waves (pump, probe and readout) are inherently coherent. Therefore, the new scheme overcomes the relative frequency fluctuations among multiple waves and ensures a much higher precision than previous schemes in the measurement of Brillouin dynamic grating spectrum (DGS) as well as Brillouin gain spectrum (BGS). The new scheme can also provide higher speed in the measurement of BGS and DGS since the time-consuming averaging process is not necessary.

Utilizing the one-laser scheme with Brillouin optical correlation domain analysis (BOCDA) technique [7,8], distributed discrimination of strain and temperature is also achieved successfully with high accuracy. In this aspect, the new scheme avoids the difficulty of strict synchronization in simultaneous frequency modulations of pump, probe, and readout waves, which is required in previous two-laser scheme [7,8] as explained in detail in Appendix. Therefore, the one-laser-based scheme is also superior to the previous studies from the view point of configuration complexity and cost, because a single function generator is sufficient in the one-laser-based scheme to provide synchronized simultaneous frequency modulations to all the three waves.

## 2. Principle and experimental setup

Figure 1 shows the experimental setup of one-laser-based generation and detection of BDG in a PMF. A 1549-nm distributed-feedback laser diode (DFB-LD) serves as the laser source. A 40-GHz intensity modulator (IM2) driven by a radio frequency synthesizer (RF2 at  $\nu_{RF2}$ ) with a proper dc bias is used to generate double sidebands with suppressed carrier (DSB-SC). The output of IM2 is launched into a fiber Bragg grating (FBG) through a circulator. The light reflected from the FBG, after further filtered by a tunable band-pass filter (TBF1), is used as the light source for pump and probe waves to write Brillouin dynamic grating. After amplified by an erbium-doped fiber amplifier (EDFA1), the light is divided into the pump and probe waves. The frequency of the probe wave is down-shifted by a single-sideband modulator (SSBM) driven by another synthesizer (RF1 at  $\nu_{RF1}$ ); the pump is chopped by IM1 for lock-in detection. The pump and probe waves are linearly polarized along the  $x$ -axis (slow-axis) of the PMF, which is used as the sensing medium. On the other hand, the light passing through the FBG is used as the readout wave to interrogate the BDG. The readout wave is  $y$ -polarized and launched into the PMF in the same direction as the pump wave.

Figure 2 illustrates an example of the measured optical spectra of the DSB-SC signal with  $\nu_{RF2} = 22\text{GHz}$ . Figure 2(a) shows the case that the DFB-LD is driven by a dc current to generate and detect BDG in the entire length of the PMF. Figure 2(b) denotes the case that a sinusoidal frequency modulation with modulation depth  $\Delta f = \sim 8.5\text{GHz}$  is applied to the DFB-LD for distributed generation and detection of DGS along the PMF based on BOCDA technique [7,8].

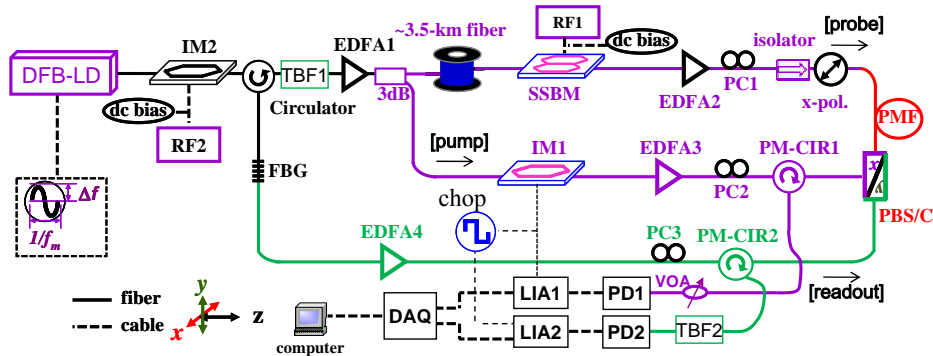


Fig. 1. Experimental setup of one-laser-based Brillouin dynamic grating generation/detection and discrimination of strain and temperature based on BOCDA. The light from DFB-LD is intensity-modulated to generate two sidebands with suppressed carrier. The lower sideband (through TBF1) is used as the source of pump/probe to generate (and measure) SBS, and to write Brillouin dynamic grating; the upper sideband (through FBG) is used as the readout wave to measure the spectrum of the Brillouin dynamic grating. The abbreviations are explained in the text body.

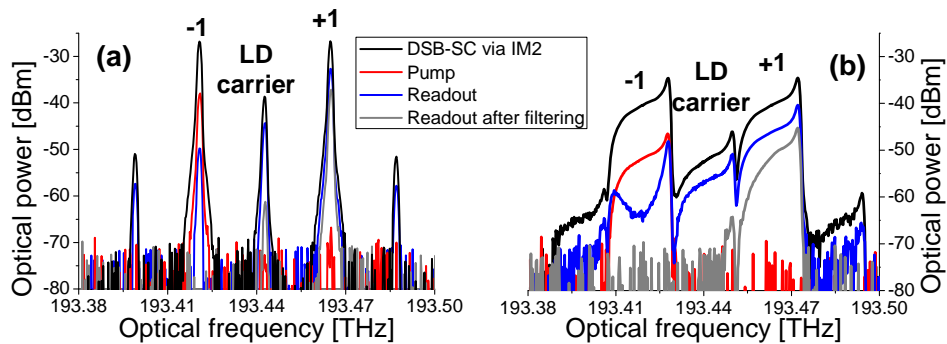


Fig. 2. Optical spectra of DSB-SC signal, pump and readout waves. (a) the DFB-LD is driven by a dc current; (b) a sinusoidal frequency modulation is applied to the DFB-LD. Gray curves denote the readout wave after passing an optical filter.

It can be seen from Fig. 2 that, thanks to twice filtering (by FBG and TBF1), the pump wave has only the component sitting away from the LD carrier by  $\nu_{RF2} = 22\text{GHz}$  (i.e.,  $-1$  order component of DSB-SC signal). The readout wave comprises dominantly  $+1$  order component, and partially suppressed carrier and  $-1$  order component due to incomplete filtering property of the FBG. The suppressed carrier and  $-1$  order component can be further cut by using an additional filter. As an example shown in Fig. 2, the readout wave including only  $+1$  order component is obtained by using the filter. We put the filter (TBF2) in the path of the diffracted readout wave. Placed at this position, TBF2 cannot only work for the above purpose but also filter out the probe/pump wave leakage along the PMF due to its finite polarization extinction ratio. The pump and readout waves are separated in frequency by  $2\nu_{RF2} = 44\text{GHz}$ . Both the amplified probe in SBS process and diffracted readout wave by the BDG are detected by photo-detectors (PDs) and demodulated by lock-in amplifiers (LIAs).

### 3. Experimental results

At first, the Brillouin frequency ( $\nu_B$ ) was obtained through the BGS measurement with RF1 swept around  $\nu_B$  [8]. Then, RF1 was fixed at the measured  $\nu_B$  so that BDG was maximized. We can measure the DGS by simply ramp-sweeping RF2. Thanks to the high stability (tens of

kHz) of RFs, the DGS (BGS as well) can be precisely measured with low frequency fluctuation.

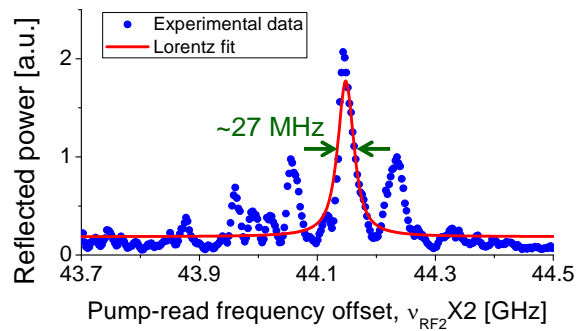


Fig. 3. Measured DGS in a 5-m PMF showing a main peak with 27-MHz linewidth and several subtle peaks with discrete  $f_{yx}$ . In comparison, previous works gave only one broad peak with 200~300-MHz linewidth. Dots, experimental data; solid curve, Lorentz fitting to the experimental data.

Figure 3 shows the measured DGS in a ~5-m-long PMF, where the dots correspond to the experimental result and the solid curve to the Lorentz fitting. It is shown that the DGS in the ~5-m PMF has a main peak with 27-MHz linewidth, which is similar to the linewidth of Brillouin scattering (20-40 MHz), and several subtle peaks with discrete  $f_{yx}$ . While in previous works [2,4,6,7,9], the DGS was shown having only one broad peak with linewidth of 200~300 MHz, which could be attributed to the relative frequency fluctuation between multiple individual laser sources. The physical reason of the multiple-peak property shown in Fig. 3 is possibly slightly-irregular birefringence of the PMF during fiber fabrication.

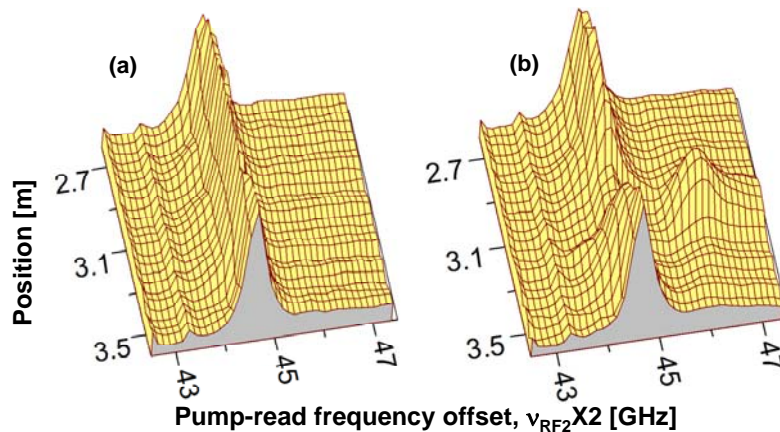


Fig. 4. Measured 3-D distribution of DGS of a PMF when (a) the entire fiber was in loose state, (b) a ~14-cm portion at 3.1-m location was strained by  $\epsilon = 2000 \mu\epsilon$ .  $T = 25^\circ\text{C}$ .

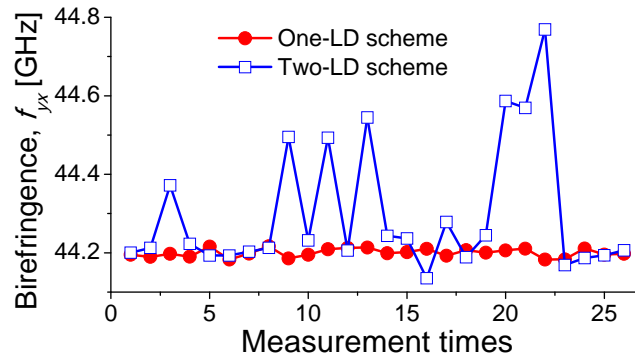


Fig. 5. Comparison of DGS measurement accuracy between one-laser scheme and two-laser scheme.

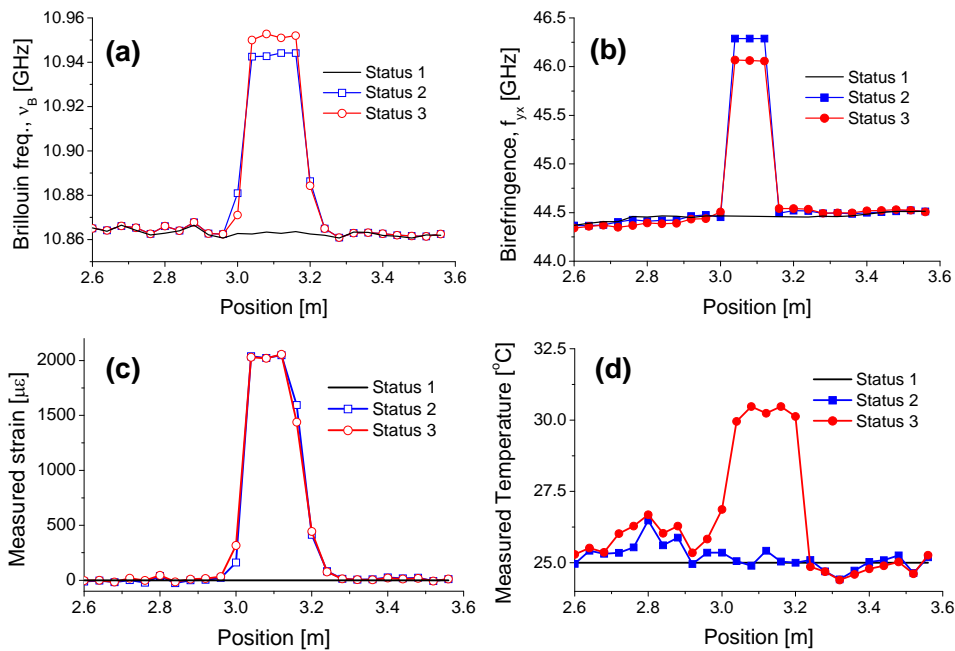


Fig. 6. Measured distribution of Brillouin frequency  $\nu_B$  (a) and birefringence-determined frequency deviation  $f_{yx}$  (b). Discriminated distribution of strain (c) and temperature (d). Solid lines (Status 1):  $T = 25^\circ\text{C}$ ,  $\varepsilon = 0 \mu\text{e}$ ; squares (Status 2):  $T = 25^\circ\text{C}$ ,  $\varepsilon = 2000 \mu\text{e}$ ; circles (Status 3):  $T = 30^\circ\text{C}$ ,  $\varepsilon = 2000 \mu\text{e}$ .

Next, we study the performance of distributed measurement of BGS and DGS based on BOCDA. In the previous two-laser scheme [7,8], sophisticated synchronous control of the frequency modulations to two DFB-LDs is necessary and it takes quite long time for getting ready to start next-position measurement. In contrary, in our new scheme, the pump/probe and readout waves are strictly coherent and originated from the same DFB-LD with the same sinusoidal frequency modulation. Distributed measurement of DGS (BGS as well) can be basically continuously performed.

The modulation frequency ( $f_m$ ) for the DFB-LD is scanned from 20080.0 kHz to 20081.6 kHz with a 64-Hz step, which corresponds to locations in PMF from 2.6 m to 3.6 m with 4-cm step. The modulation depth ( $\Delta f$ ) is set to be 1 GHz for BGS measurement and 6 GHz for DGS measurement, respectively. According to [7], the measurement range is  $d_m =$

5 m; the nominal spatial resolution of BGS measurement is  $\Delta z_B = \sim 5$  cm and that of DGS measurement is  $\Delta z_D = \sim 10$  cm, respectively. The total measurement time for both BGS and DGS at one position is less than 2 s.

Figure 4 illustrates measured three-dimensional distribution of DGS, where in Fig. 4(a), the entire fiber was in loose state; in Fig. 4(b), an axial strain ( $\varepsilon = 2000 \mu\varepsilon$ ) was applied upon a 14-cm long portion at the location of 3.1 m. The strain-induced increase of the birefringence-determined frequency deviation ( $f_{yx}$ ) can be clearly observed. We repeated the DGS measurement at the same location, and compared the accuracy of this scheme with respect to that of the previous two-laser based scheme. As shown in Fig. 5, the  $f_{yx}$  measured in this new scheme shows high stability and accuracy (several MHz), while that obtained by the two-laser scheme suffers very high fluctuation (several hundreds of MHz).

By peak-searching of the distribution of the measured BGS and DGS along the fiber, we obtain the distribution of the  $\nu_B$  and  $f_{yx}$ . Figure 6 summarizes the experimental results when the fiber was heated from 25 °C to 30 °C or/and the strain ( $\varepsilon = 2000 \mu\varepsilon$ ) was applied both at the location of 3.1 m. It is clear that the imposed strain increases both the  $\nu_B$  and  $f_{yx}$ , while the heating has a contribution to the  $f_{yx}$  opposite to that to the  $\nu_B$ . By referring to the strain and temperature coefficients of the  $\nu_B$  and  $f_{yx}$  [6], we evaluated the distribution of the temperature and strain along the fiber. The results summarized in Fig. 6(c) and 6(d) match well with the setting situation. There is a slight variation in the temperature around 3.1 m, which is possibly due to the poor performance of heating unit. Compared to the previous two-laser scheme [8], the one-laser scheme demonstrated here has the similar spatial resolution ( $\sim 10$  cm) and measurement range ( $\sim 5$  m), but have several advantages including faster measurement speed without time-consuming averaging, simpler measurement without sophisticated synchronization, and higher accuracy as shown in Fig. 5.

#### 4. Conclusion

We demonstrated a novel scheme to generate and detect Brillouin dynamic grating in a PMF by use of one-laser source. Thanks to the strict coherent nature among the pump/probe and readout waves originated from the same laser source, both DGS and BGS can be measured with high accuracies. Compared to the previous two-laser scheme, it is much easier and faster to measure the BGS and DGS distribution, i.e., to discriminate the strain and temperature distribution.

When applying this one-laser scheme to BOCDA, the modulation depth of the sinusoidal frequency modulation to the DFB-LD, which determines the effective sensing number [7], should be smaller than one quarter of the birefringence-determined frequency deviation because of the spectrum-overlapping of the pump and readout waves [see Fig. 2(b)]. This issue can be improved by using a PMF with greater birefringence as used in Ref [2]. The measurement range of this novel scheme can easily be extended by incorporating a kind of temporal gating scheme, which is currently under study.

#### Appendix

Figure A1 illustrates dispersion properties of all four waves during the generation and detection of BDG in a PMF, including writing light waves (pump and probe), reading light wave (readout) and acoustic wave (dynamic grating as well). All pump, probe and readout waves follow the rule of optical dispersion property, given by

$$\omega_{op} = c \cdot |\beta_{op}|,$$

where  $\omega_{op}$  is the angular frequency of the light waves,  $c$  is the light speed in vacuum, and  $\beta_{op}$  ( $= 2\pi/\lambda \cdot n_{\text{eff}}$  with  $\lambda$  the wavelength) is the propagation constants of the light waves. The acoustic wave satisfies the rule of acoustic dispersion property, given by

$$\omega_{ac} = V_a \cdot |\beta_{ac}|,$$

where  $\omega_{ac}$  ( $=2\pi \cdot \nu_B$ ) is the angular frequency,  $V_a$  is the velocity, and  $\beta_{ac} = 2|\beta_{op}|$  is the propagation constant, in which the factor of 2 is attributed to SBS Bragg condition [1], of the longitudinal acoustic wave.

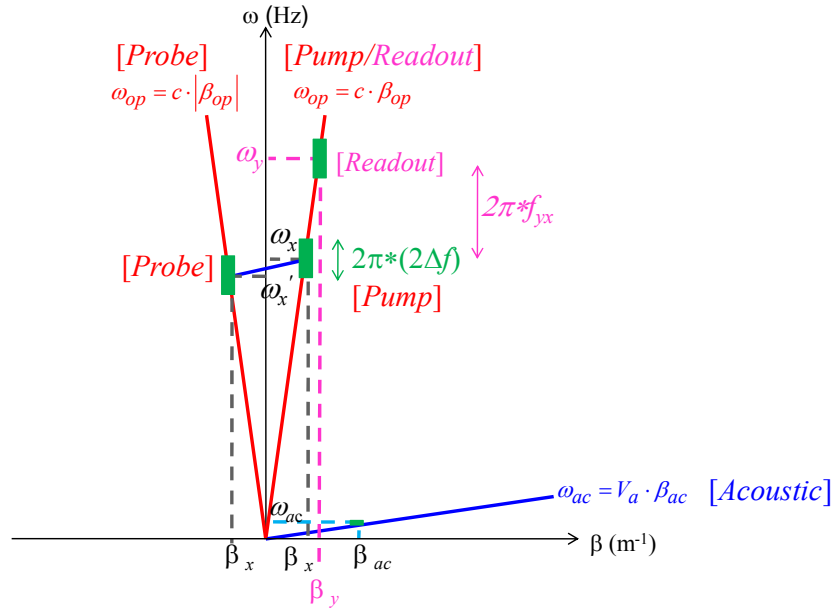


Fig. A1. Dispersion properties of all pump, probe and readout waves together with acoustic wave (Brillouin dynamic grating).

The difference of the effective refractive indexes (i.e., the birefringence  $B = n_{eff}^x - n_{eff}^y$ ) along the orthogonal principal axes in the PMF differentiates the propagation constants between the  $x$ -polarized pump wave and  $y$ -polarized readout wave. To compensate this difference occurring in SBS Bragg condition, that is,  $n_{eff}^x/\lambda_x * 2V_a = n_{eff}^y/\lambda_y * 2V_a$ , the frequency of the readout wave ( $y$ -polarized) should be larger than that of the pump wave ( $x$ -polarized) by the birefringence-determined frequency deviation ( $f_{yx}$ ) [2,4,6]. When a sinusoidal frequency modulation with modulation depth ( $\Delta f$ ) in Brillouin optical correlation domain analysis (BOCDA) technique is applied to the pump and probe waves, as shown in green squares in Fig. A1, the acoustic wave (Brillouin dynamic grating) is locally generated in the correlation peak [7]. Because of the huge contrast ( $\sim 5 \times 10^4$ ) between the light speed ( $c$ ) and the acoustic velocity ( $V_a = \sim 6000$  m/s), the change of the Brillouin frequency ( $\delta\nu_B = 2V_a * n_{eff}/c * \Delta f$ ) due to the sinusoidal frequency modulation to the pump/probe wave can be omitted (for example,  $\delta\nu_B = \sim 0.58$  MHz for  $\Delta f = 10$  GHz). However, the readout wave follows the same dispersion property as the pump wave, which is totally different from the case of the acoustic wave. It is the physical reason why a simultaneous frequency modulation synchronous to the frequency modulation applied to the pump/probe wave has to be applied to the readout wave as illustrated in the green square in Fig. A1.

### Acknowledgments

This experimental study was finished at The University of Tokyo. This work is supported by the ‘‘Grant-in-Aid for Scientific Research (S)’’ and the ‘‘Global Center of Excellence Program (G-COE)’’ from the Ministry of Education, Culture, Sports, Science and Technology, Japan.

Weiwen Zou is grateful for the support from the National Natural Science Foundation of China (Grant No. 61007052).